Early stages of development in Mediterranean red coral (Corallium rubrum): The key role of sclerites

Bruna Giordano, Lorenzo Bramanti, Jonathan Perrin, Ozan Kahramanoğulları, Daniel Vielzeuf

frontiers | Frontiers in Marine Science

TYPE Original Research
PUBLISHED 06 February 2023
DOI 10.3389/fmars.2023.1052854

OPEN ACCESS

EDITED BY
Nozomu Iwasaki,
Rissho University, Japan

REVIEWED BY
Fiorella Prada,
Rutgers, The State University of New Jersey, United States
Yannicke Dauphin,
Muséum National d'Histoire Naturelle, France

*CORRESPONDENCE
Bruna Giordano
bruna.giordano@unica.it

†These authors have contributed equally to this work and share senior authorship

SPECIALTY SECTION
This article was submitted to Marine Biology, a section of the journal Frontiers in Marine Science

RECEIVED 24 September 2022
ACCEPTED 13 January 2023
PUBLISHED 06 February 2023

CITATION
Giordano B, Bramanti L, Perrin J, Kahramanoğulları O and Vielzeuf D (2023) Early stages of development in Mediterranean red coral (*Corallium rubrum*): The key role of sclerites. *Front. Mar. Sci.* 10:1052854. doi: 10.3389/fmars.2023.1052854

Early stages of development in Mediterranean red coral (*Corallium rubrum*): The key role of sclerites

Bruna Giordano[1,2,3*], Lorenzo Bramanti[3†], Jonathan Perrin[4], Ozan Kahramanoğulları[5] and Daniel Vielzeuf[6†]

[1]Department of Life and Environmental Sciences, University of Cagliari, Cagliari, Italy, [2]Department of Environmental Biology, Sapienza University of Rome, Rome, Italy, [3]Laboratoire d'Ecogéochimie des Environnements Benthiques, LECOB, Observatoire Océanologique de Banyuls sur Mer Centre National de la Recherche Scientifique (CNRS)-Sorbonne Université, Banyuls sur Mer, France, [4]Anatomix Beamline, Synchrotron SOLEIL, Saint Aubin, France, [5]Faculty of Computer Science, Free University of Bolzano-Bozen, Bolzano, Italy, [6]Aix Marseille Univ, Centre National de la Recherche Scientifique (CNRS), Centre Interdisciplinaire de Nanoscience de Marseille (CINAM), Marseille, France

Corals are ecosystem engineers whose tree-like structures give three-dimensional complexity to the habitat. Their population dynamics are affected by recruitment and juvenile survival. Therefore, several defense strategies, such as the formation of hard skeletons and/or spicules, have evolved to protect these vulnerable stages. The family Coralliidae, to which "precious corals" belong, represent an exception in the order Scleralcyonacea, as they form hard $CaCO_3$ skeletons and small $CaCO_3$ structures, the sclerites. The skeletogenesis of *Corallium* species is relatively well documented in adult colonies but remains poorly known in the early stages of the development of new colonies. To shed light on the timing of *Corallium rubrum*'s early skeleton formation and the role of sclerites, we focused on the first 4-years of life, applying different techniques, from scanning electron microscopy to synchrotron tomography and laser ablation inductively coupled plasma-mass spectrometry. Our results show that: 1) the first visible sclerites in the primary polyp appear at least 12 days after larval settlement, which is associated with a high $CaCO_3$ production rate (4.5 ± 2.3 µg of $CaCO_3$ per day). Furthermore, growth rings are visible in the sclerites, showing that fully matured sclerites grow fast, probably in 3 to 4 days. 2) Sclerites are the only biomineral product in the first year of life of *C. rubrum*'s colonies. 3) The evidence of a consolidated axial skeleton, intended as the inner part of the skeleton characteristic of the adult red coral (the medullary zone, MZ), is recorded for the first time in 2-year-old colonies. 4) The annular zone (AZ) around the medullary zone starts forming not before four years after settlement. Thus, primary polyp builds a deformable armor made of only sclerites during the first year. This shelter provides mechanical protection from abrasion and predation to early settled colonies. After two years, settlers are firmly and mineralogically attached to the substratum, which makes them less vulnerable to predation than younger recruits that are not anchored by the skeleton.

KEYWORDS

***Corallium rubrum*, early life stages, recruitment, biomineralization, skeletogenesis, sclerites, skeleton**

1 Introduction

Biomineralization is a common biological process, and several groups of marine invertebrates (e.g., sponges, mollusks, and echinoderms) produce mineral structures with various functions. Among these, the biomineralization of corals (Cnidaria: Anthozoa) holds an important ecological significance, as it can form vast 3D frameworks such as coral reefs, which enhance environmental structural and morphological complexity (Rossi et al., 2017). Within Anthozoa, Scleractinian corals build a massive skeleton of aragonite. In contrast, in most Octocoral species, the axial skeleton is proteinaceous, and the biomineral component is represented by the sclerites, small $CaCO_3$ structures embedded in the coenenchyma, the tissue surrounding the axial skeleton (Bayer, 1955; Bayer, 1957). Among Octocorals, the family Coralliidae, which includes precious coral species such as the Mediterranean red coral (*Corallium rubrum*), represents an exception as its members do not build a proteinaceous skeleton, but two types of magnesian calcite structures: (1) a hard-branched axial skeleton and (2) sclerites, also referred to as spicules (Lacaze-Duthiers, 1864).

The target species of this study, *C. rubrum*, is an emblematic octocoral, mainly distributed in the western Mediterranean basin at depths ranging from 10 to 1000 m (Costantini et al., 2010). Because of the high value of its skeleton in the jewelry market, it has been the object of intense fishing, which brought several populations to overexploitation and local extinction, causing conservation concerns. The main morphological features of *C. rubrum* have been first described by Lacaze-Duthiers (1864) in his seminal monography on this species (for a thorough critical review of Lacaze-Duthiers' work, see Vielzeuf et al., 2022). *C. rubrum* is a gonochoric brooder species that releases lecithotrophic, aposymbiotic, ciliated larvae between July and the first half of August (Lacaze-Duthiers, 1864; Santangelo et al., 2003; Bramanti et al., 2005). After its free-living period (a few days), larvae find a suitable substrate (Zelli et al., 2020), where they firmly attach and undergo the metamorphosis process which implies extensive tissue remodelling. This process leads to the formation of the primary polyp. After less than one year, the primary polyp starts budding and produces genetically identical polyps that form the coral colony. *C. rubrum* is composed of a rigid, red, primarily inorganic axial skeleton coated with coenenchyma. The mesoglea, a collagen-like substance included between the ectodermal and endodermal layers of the coenenchyma, contains sclerites that give a granular appearance to the living tissues (Lacaze-Duthiers, 1864; Grillo et al., 1993). Both kinds of skeletal structures -axial skeleton and sclerites- are made of Mg-rich calcite with a small percentage of organic components (Grillo et al., 1993; Allemand et al., 1994). *C. rubrum* sclerites are red, small (60-80 μm), and slightly elongated structures that generally display a dumbbell shape (Lacaze-Duthiers, 1864; Floquet and Vielzeuf, 2011). Concerning the internal structure of the adult axial skeleton, two distinct areas are observed: 1) a central cross-shaped medullar zone (MZ) and 2) a surrounding annular zone (AZ) constituted by several concentric calcitic layers (Lacaze-Duthiers, 1864; Marschal et al., 2004; Vielzeuf et al., 2008; Vielzeuf et al., 2013; Perrin et al., 2015; Vielzeuf et al., 2018). Several studies suggested that the skeletal axis results from two distinct growth mechanisms: the "block by block" growth for the MZ and the "layer by layer" growth for the AZ (Grillo et al., 1993; Allemand and Bénazet-Tambutté, 1996; Debreuil et al., 2011; Perrin et al., 2015; Vielzeuf et al., 2018). The "block by block" growth consists of the addition of sclerites, or sclerite aggregates, cemented together to form the inner core of the skeleton. In contrast, the "layer by layer" growth is characterized by radial growth resulting from the addition of concentric layers of calcite secreted by the aboral ectoderm with scarce inclusion of sclerites (Perrin et al., 2015). These two distinct growth processes are associated with different growth rates and kinetics being the axial growth almost ten times faster than the annular one [axial growth 1.8 ± 0.7 mm $year^{-1}$ (average ± SD; Garrabou and Harmelin, 2002), annular growth 0.1-0.4 mm $year^{-1}$ (average ± SD; Abbiati et al., 1992; Garrabou and Harmelin, 2002; Marschal et al., 2004; Gallmetzer et al., 2010; Priori et al., 2013; Vielzeuf et al., 2013; Bramanti et al., 2014)].

While it is widely accepted that the axial skeleton's function (i.e., evolutionary advantage) is to support the colony and optimize the food capture of the polyps, the function of sclerites is debated. According to Lewis and Wallis (1991), sclerites have a role in gorgonian bending capacities. Kingsley (1984) proposed several functions for sclerites in the gorgonian *Leptogorgia virgulata*, including a sensory function, enhancement of stability, protection against predators, and mechanical protection against abrasion. Allemand and Bénazet-Tambutté (1996) suggested that one of the main functions of *C. rubrum* sclerites is the mechanical protection against abrasion in adult colonies. Finally, Perrin et al. (2015) suggested that sclerites in the coenenchyma could act as nuclei that are progressively trapped and cemented together to extend the tip in the proximal branches of adult colonies. However, since multi-functionality is a common feature in biominerals (Lowenstam and Weiner, 1989), it would not be surprising if sclerites had other functions.

Most studies conducted on the biomineralization of *C. rubrum* focused on adult stages (Conci et al., 2021), and rarely considered recruits (0-1-year-old) or juveniles (1-4-year-old). From a conservation and restoration perspective, deepening the knowledge of the biology and ecology of early life stages is crucial to better understand the vulnerability and primary threats of these stages, known to be sensitive and exposed to various menaces such as competition, predation, and other abiotic disturbances. In this context, sclerites' role in the growth and survival of young recruits has not yet been examined. More generally, besides the pioneering work of Lacaze-Duthiers (1864), little is known about the mechanisms and timing of the skeleton formation in young red coral colonies. Hence, the objective of the present study is to describe the early stages of skeleton development in *C. rubrum*, focusing on assessing the timing of 1) sclerites' production, 2) sclerites' aggregation ("block by block" growth), 3) radial accretion ("layer by layer" growth). The final aim is to shed light on the role of sclerites in the growth and survival of newly settled colonies. For this purpose, we observed newly settled red coral individuals from the moment they were attached to the substrate. We used a large panel of instruments (binocular and polarizing microscope, scanning electron microscope, synchrotron tomography, laser ablation inductively coupled plasma-mass spectrometry LA-ICPMS) to describe the growth process on *C. rubrum* colonies at different ages (from 17

days to 4-year-old) settled and developed in the natural environment or aquarium tanks.

2 Materials and methods

2.1 Sampling

2.1.1 Aquarium samples

The age of *C. rubrum* colonies used for the measurements spanned from 17 days to 4 years, considering the age of corals' recruits from the larval settlement. Samples were divided into seven classes (17 days, 1, 3, 8 months, 1, 2, and 3-4 years) and analyzed with different techniques (see Table 1 for a summary of analyzed samples). The first age class (17 days) was determined based on the first observation of sclerites in the polyp. The last age class (3-4 years) represents the upper limit of the juvenile age class (i.e., the start of the layer-by-layer growth mode). As the sampling is destructive, the choice of the age classes represents a tradeoff between sampling frequency and availability of individuals. The youngest samples were obtained from larvae settled and developed in aquarium tanks under controlled conditions (17 days to 12-month-old recruits) or *in situ* (24-month-old recruits). The oldest samples (3 to 4-year-old) were obtained by *in situ* settlement on artificial substrates from a previous study (see Bramanti et al., 2005 for details). All the samples were dried alive to be subsequently analyzed.

For their reproduction in aquaria, sexually mature *C. rubrum* colonies (> 7 mm basal diameter) were collected in early July 2018 and 2019 (45 colonies in 2018, 21 and 24 females and males, respectively; 35 colonies in 2019, 20 and 15 females and males, respectively), just before spawning (Santangelo et al., 2003) between 25 and 35 m depth by SCUBA-diving, in the area adjacent to the Marine Reserve Cerbère/Banyuls (North-Western Mediterranean Sea, France). Collected colonies were transferred in five open circuit aquaria with an air bubbling system and maintained at 16–18°C. The sex of each colony was determined by microscope observations (Santangelo et al., 2003). The corals were re-distributed in five closed-circuit aquaria to mix female and male colonies and ensure oocytes fertilization. The aquaria were surveyed daily for larval release, which began late July-early August (August 5th, 2018; July 22nd, 2019). *C. rubrum* larvae were transferred in 3 new closed circuit, air-bubbled, and temperature-controlled aquaria and offered settlement substrates. All the aquaria were illuminated by two LED white lights with 12 h light – 12 h dark cycles (Zelli et al., 2020 for details). After larval settlement and metamorphosis into polyps, all the colonized substrates were transferred to other open circuit aquaria with an air bubbling system and kept at constant temperature and pH to reproduce the values recorded *in situ* (16–18°C and 8.0-8.1 for temperature and pH, respectively). Young samples were collected at different developmental stages throughout the first year of the experiment. The youngest samples, aged 17 days, were collected a few days after the beginning of sclerite production, while other samples were collected at 1, 3, 8, and 12 months after settlement.

2.1.2 *In situ* samples

A system of artificial caves near the Cerbére/Banyuls Marine Reserve (at 30 m depth) was used to obtain 24-month-old colonies. Adult colonies were implanted in 2017 in the vault of the artificial caves. In 2018, larvae settled on terracotta plates (20x20cm) positioned upside down on the vault, and samples were collected in 2020. Other samples, settled on marble tiles and grown in situ, were obtained from previous research (Bramanti et al., 2005 for details).

TABLE 1 List of the analyzed samples, divided into age classes.

Age class	Number of samples	Growth environment	Analysis
17 days	2	ex situ	Stereomicroscope SEM
1 month	5	ex situ	Stereomicroscope SEM Synchrotron tomography
3 months	10	ex situ	Stereomicroscope SEM Synchrotron tomography
8 months	4	ex situ	Stereomicroscope SEM Synchrotron tomography
1 year	9	ex situ	Stereomicroscope SEM Synchrotron tomography
2 years	10	in situ	Stereomicroscope SEM Synchrotron tomography
3-4 years	7	in situ	Stereomicroscope SEM Synchrotron tomography LA-ICPMS

For each class, the number of samples, the growth environment, and the analysis performed is indicated. *Ex situ* refers to aquarium tanks while *in situ* refers to natural environment.

The age of the juveniles, ranging from 1- to 4-year-old, was calculated based on their basal diameters. The oldest samples were merged into a single 3- to 4-year-old class to avoid errors in age estimation due to different measurement methods between Bramanti et al. (2005) and the present work.

2.2 Determination of sclerite production and aggregation

Early settled recruits, maintained in aquarium tanks, were observed daily and photographed with a high-resolution camera mounted on a Zeiss Scope.A1 to assess the date of appearance of sclerites produced by the primary polyp, i.e., the first polyp metamorphosed and developed after the larval settlement. In addition, two early recruits (17 days old) were collected and observed by SEM in secondary electron mode (see below for details) to estimate the number of sclerites produced by the primary polyp. For each recruit, the number of sclerites was counted three times on the same SEM image. The average number of sclerites (± MAE) and the $CaCO_3$ deposition rate (µg/day) produced by the primary polyp were estimated, considering that the mass of a single sclerite is about 0.16 ± 0.08 µg (Allemand and Grillo, 1992).To establish the beginning of the sclerites' aggregation process ("block by block" growth, when sclerites start being cemented together), we observed and photographed all the samples recovered from the aquaria and subsequently dried, firstly by stereomicroscope (Zeiss Scope.A1), and then by scanning electron microscope (SEM) and synchrotron tomography.

2.2.1 Scanning electron microscope

External morphology and internal structure of the recruits were observed with a field-emission scanning electron microscope (Raith Pioneer at CINaM, Marseille), using secondary electrons (SE) and backscattered electrons (BSE), respectively. All the samples were carbon-coated before the observations. The operating conditions for SE images were 10 kV accelerating voltage and 6 to 15 mm working distance. BSE images were taken on polished sections embedded in epoxy, with 20 kV accelerating voltage, 3 to 4 nA probe current, 6.6 mm working distance, and aperture of 120 µm. In BSE mode, the image contrast mostly depends on the sample composition: high average atomic number materials appear brighter than low-Z materials, and holes appear in black, highlighting chemical variations on polished skeleton surfaces.

2.2.2 Micro-X-ray tomography

Micro-X-ray tomography (performed at synchrotron SOLEIL, Saint-Aubin) is a non-destructive method for studying the structure of several types of materials, including organic tissues and biominerals. It allows visualizing samples in three dimensions, with a high spatial resolution (<1 µm). A white beam was used with 100 and 200 µm of copper as a filter, resulting in 20-25 KeV energy. A large field detector with an ORCA Flash v4 camera and Hasselblad objective 2x results in a pixel size of 3.25 µm and a field of view of 6.65 mm. For the 10x magnification, the revolver detector with a 10x Mitutoyo objective and the ORCA Flash v4 camera results in a pixel size of 0.65 µm and a field of view of 1.33 mm. Single and half acquisitions were used, consisting of 2000 and 4000 projections between 0-180° and 0-360° rotation, respectively. The 3D reconstruction of the images was performed with the PyHST.2 software. 3-D models were processed with ImageJ to extract orthogonal and transversal slices and AvizioLite software for three-dimensional rendering (Weitkamp et al., 2017; Weitkamp et al., 2018).

2.3 Determination of the transition from "block-by-block" to "layer-by-layer" mechanism of growth

To assess if the "layer by layer" growth, characteristic of the annular zone, already occurs in the oldest samples (3–4-year-old colonies), we analyzed the chemical signature of the samples through a trace element analysis by LA-ICPMS. A principal component analysis (PCA) was then used to compare our measurements with those published by Vielzeuf et al. (2018), which showed systematic differences in trace elements composition (Li, Na, Mg, Sr, U) between annular and medullar zone in adult colonies.

2.3.1 Laser ablation inductively coupled plasma mass spectrometry (LA-IPCMS)

LA-IPCMS was applied on two 3–4-year-old sections previously observed by the SEM. Trace element concentrations in *C. rubrum* skeletons were determined on an Agilent 7500 cs ICPMS coupled to a 193 nm Excimer Resonetics M-50E laser ablation system with maximum output energy of 6 mJ (Laboratoire Magmas et Volcans, Clermont-Ferrand). Analyses were performed with a laser pulse frequency of 3 Hz and a constant beam diameter of 33 µm. The ablated material was carried by helium (0.7 L/min) and mixed with nitrogen and argon in front of the ICP. The following isotopes were collected: $_{7}$Li, $_{23}$Na, $_{24}$Mg, $_{31}$P, $_{39}$K, $_{53}$Cr, $_{55}$Mn, $_{66}$Zn, $_{88}$Sr, $_{137}$Ba, $_{208}$Pb, and $_{238}$U, with integration times varying between 30 and 200 ms depending on the element. Typical minimum detection limits are 0.1, 1.6, 0.1, 8.5, 2.3, 1.8, 0.8, 0.6, 0.05, 0.3, 0.07, and 0.03 µg/g for Li, Na, Mg, P, K, Cr, Mn, Zn, Sr, Ba, Pb, and U, respectively. Internal instrumental errors are close to 0.2, 160, 1030, 30, 5, 0.7, 0.4, 0.4, 90, 0.4,0.05, and 0.02 µg/g, respectively. The mean calcium abundance measured by EMP for a series of coral samples was used as an internal standard. A typical signal acquisition consisted of collecting a background signal for 30 s followed by laser firing for 70 s. Trace-element reductions were made with the Glitter software (van Achterbergh et al., 2001). The long firing time (70 s) allowed to check (1) the stability of the signal during the measure (flat plateau) and (2) the presence of voids or inclusions during firing. Only flat plateau portions were processed, and initial spikes or signals associated with surface contamination were discarded. The NIST 610 glass was used as an external standard (Shaheen et al., 2008). The glasses NIST 612 and BCR-2G (Gao et al., 2002) were also analysed to check the accuracy and precision of the analyses.

3 Results

3.1 Sclerite production- first steps towards the formation of a flexible proto-skeleton

3.1.1 Recruits (< 1 year)

A total of twenty-one recruits, ranging from 17 days old to 8 months old, were studied. The first sclerites were detected in the primary polyp 12 days after larval settlement. Sclerite production in settled individuals is associated with a change in color (from white to light pink), which attests the first appearance of small red spicules in the whitish organic tissues of the primary polyp (Figures 1, 2A). The presence of sclerites is confirmed by stereomicroscope and SEM observations (Figure 3A).

The number of sclerites produced by a 17-days-old recruit, estimated by counting sclerites on high spatial resolution SEM images, was 461 ± 6 (average ± MAE) (Figure 3A). The mass of a single sclerite is about 0.16 ± 0.08 µg (Allemand and Grillo, 1992) therefore a single polyp can produce 76.3 ± 39.2 µg of CaCO3 in 17 days, which results in a $CaCO_3$ deposition rate of approximately 4.5 ± 2.3 µg day^{-1}. It is worth noting that 12 days are sufficient to produce fully developed sclerites with their characteristic dumbbell shape (Figure 2A). Furthermore, SEM images of sclerites enclosed in 2- and 3- to 4-year-old recruits show the presence of growth rings within sclerites (Figure 2B). We observe a central core and three-four prominent growth marks within these structures, interrupted by fainter marks.

During a recruit's first year of life, the main change in its calcified structure is mainly the number of sclerites produced. This is illustrated by the SEM images (Figure 3) and in the 3D animation resulting from tomography reconstruction (Kahramanoğulları et al., 2022). In 17-day-old recruits (Figure 3A), sclerites appear fully developed, with the classical dumbbell shape, well separated and discernible from each other, forming a single layer of sclerites in the polyp. In 1-month-old recruits, a more compact structure is observed (Figure 3B), associated with an increased number and density of sclerites. At this age (1 month), a compact skeleton is still not present,

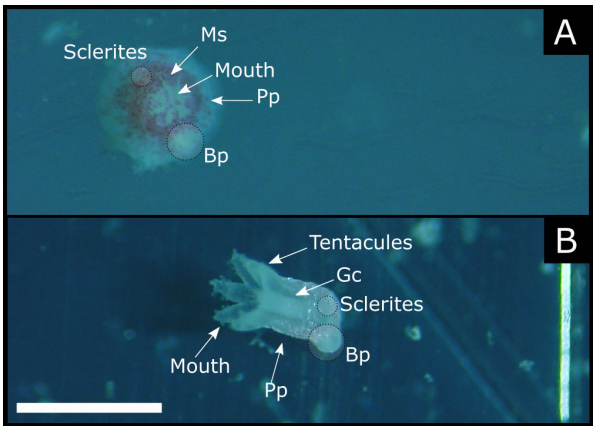

FIGURE 1
Living 1-month old recruits. **(A)** orthogonal view of the folded polyp. **(B)** lateral view of the open polyp. Ms, mesenteric septa; Pp, primary polyp; Bp, budding polyp; Gc, gastric cavity (scale bar 1 mm).

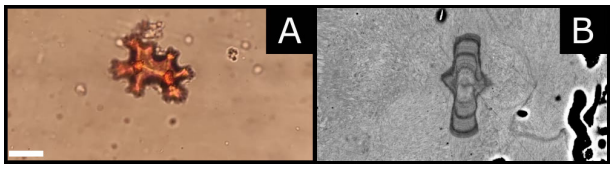

FIGURE 2
(A) Blow up of a sclerite by stereomicroscope. **(B)** Scanning electronic microscopy: backscattered electron mode. The image shows the internal structure of a sclerite found in the axial skeleton of a 3- to 4-year-old coral. It is possible to observe a central core and three dark and evident growth marks, representing the sclerite's growth rings (scale bar 9 µm).

as voids and no cemented areas appear between the sclerites. These latter are well recognizable and separated, and their density remains relatively low (Figure 3B).

3.1.2 One-year-old colonies

A total of nine 1-year-old recruits were studied. These samples are characterized by a more compact structure than younger settlers (Figure 3C). Voids at the edges and around the central core are less frequent, and the diameter of the structure is larger than in 1-month-old individuals (1-month-old basal diameter = 0.70 ± 0.20 mm; 1-year-old basal diameter = 0.92 ± 0.41 mm). Observations by stereomicroscope, SEM, and tomography (Figures 3C, D), show a cavity that should represent the primary polyp's location, with sclerites distributed within a restricted area around its base. No ongoing sclerites cementation is observed on the SEM images even though no clear separation between sclerites can be seen, probably due to the dried organic layer (the coenenchyma) covering the sample (Figure 3C). The absence of cementation is confirmed by X-ray tomography. Indeed, the tomography images show that the skeleton consists exclusively of sclerites embedded in the organic layer (Figure 3D).

Interestingly, no sclerite is present between the polyp base and the substrate. Moreover, we observed that the structure formed by the sclerites in the mesoglea does not collapse when the samples dry, preserving the shape of the cavity occupied by the polyp. Finally, our observations show that sclerite density and number increase throughout the first year without signs of cementation.

3.2 Sclerites aggregation- first stage of formation of a consolidated axial skeleton

3.2.1 Two-year-old colonies

Sclerites aggregation was investigated on ten 2-year-old samples. Stereomicroscope observations in one of those samples show at least four footprints left by the ancient polyps (Figure 4A). Sclerites are not closely concentrated around the polyps, as in the younger samples, but occupy a wide area (2.7 ± 1.1 mm) around the colony's base (Figure 4A). Three out of ten samples were observed by SEM in both SE and BSE modes. Images in SE mode show that the external surface of the one-and two-year-old samples are similar, both appearing like a pile of sclerites (Figure 4B). However, the SEM images of polished cross-sections reveal an inner structure that is significantly different

10.3389/fmars.2023.1052854

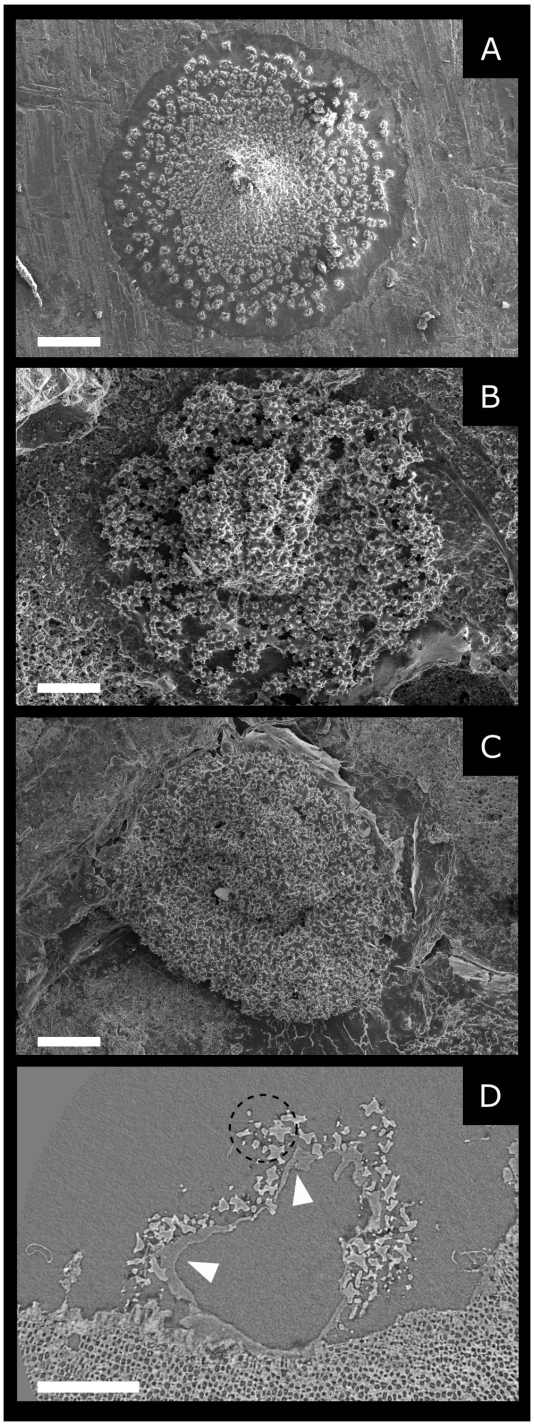

FIGURE 3
(A–C) Scanning electron microscopy: SE mode. Recruits at different ages: **(A)** 17-day-old (scale bar 300 µm). **(B)** 1-month-old (scale bar 100 µm). **(C)** 1-year-old (scale bar 150 µm). **(D)** Synchrotron tomography of 1-year-old recruit, longitudinal. The central void represents the gastric cavity delimitated by the organic tissue indicated by the white arrows. These tissues are extensively present on the aboral side of the polyp and allow the adhesion of this latter to the substrate. Sclerites (dotted circle) contour the gastric cavity (scale bar 0.2 mm).

between one- and two-year-old colonies (Figures 4C–G). In the 2-year-old colonies, an outer layer composed of sclerites is still present, but a solidified inner axial skeleton is observed for the first time.

Furthermore, a thin calcitic layer is observed at the base of the polyp in contact with the substrate (Figures 4C, F, G). BSE images (Figures 4C-E) also show that these skeletal structures are made of sclerites cemented together, much like the medullar zone of adult colonies (Debreuil et al., 2011; Perrin et al., 2015). The cement is composed of calcitic layers that can be recognized due to contrast variations in BSE images (Figure 4E) which indicate slight differences in chemical composition, confirming previous observations by Perrin et al. (2015) and Vielzeuf et al. (2018). These layers are often thin, discontinuous in space and characterized by complex geometries. It is also worth noting that the cement proportion is large compared to the proportion of sclerites. The X-ray tomography of a different colony of the same age indicates the presence of four polyps separated by thin walls made of cemented sclerites (Figures 4F, G). The tomography also allows the detection of micro-protuberances on the skeleton surface, which are tiny structures, smaller than sclerites, characterized by complex arborescent shapes and systematically observed at the surface of skeletons of adult colonies (Grillo et al., 1993; Vielzeuf et al., 2008).

3.3 Exploring the beginning of annular growth

Seven specimens were used to study the skeleton development at 3-4 years of age. Stereomicroscope observations show that similarly to what is observed in the 2-year-old colonies, the sclerites are scattered on the substrate, around the axial skeleton, forming a large base around the central core of the coral (mean diameter: 7,7 mm, continuous white line in Figure 5A). SEM observations were performed on five samples: three specimens were observed by SE mode, while BSE mode was used on two samples previously embedded in epoxy and polished. Images in SE mode show the axial skeleton and its external morphology (Figures 5B, C). Despite the poor state of preservation of the samples, micro-protuberances are observed on the skeleton surface. Images in BSE mode show that sclerites inside the skeleton are abundant over the entire section length, as in 2-year-old colonies. The growth pattern is still multidirectional and chaotic (as observed in the adult MZ) and characterized by several geometrically complex calcitic layers (Figures 5D, E). Furthermore, skeleton sections present traces of micro-protuberances, which are particularly frequent towards the external surface of the colonies. The presence of the axial skeleton is confirmed by X-ray tomography.

The skeletons of 3-4-year-old recruits are big enough to determine if layer-by-layer growth, characteristic of annular zones, has already started at this age. SEM-BSE images do not show regular growth rings (Figure 5F). Following Vielzeuf et al. (2018), we performed 38 LA-ICPMS measurements on two transverse and longitudinal sections of 3-4-year-old skeletons which revealed compositional features that mostly matched medullary zones. Four out of 38 analyses performed have Li contents slightly lower than 3 µg/g, two analyses have lower U content than 0.08 µg/g, and there is no analysis with both Li and U lower than the above-mentioned critical values (Li < 3 µg/g; U < 0.08 µg/g). As a complementary processing of the data, a PCA analysis was performed, combining the Vielzeuf et al. (2018) dataset and our measurements. These results further indicate that the chemical compositions of the 3-4-year-old

10.3389/fmars.2023.1052854

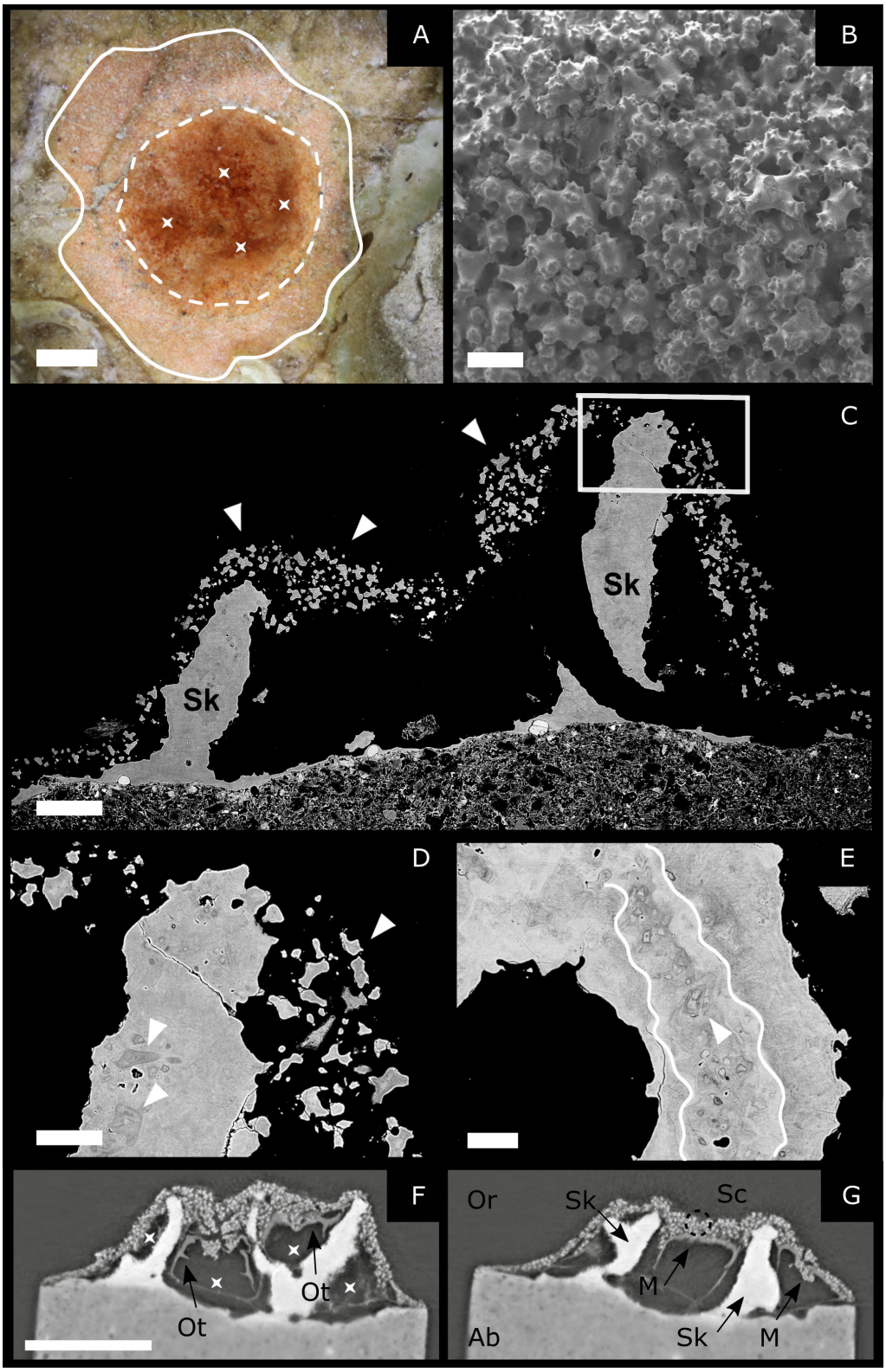

FIGURE 4
2-year-old samples. **(A)** Stereomicroscope image: asterisks indicate the four footprints left by the polyps. The white dashed lines indicate the central portion of the colony, where the polyps lay. The white, continuous line indicates the area around the colony base, where sclerites diffuse (scale bar 0.5 mm). **(B)** Scanning electron microscopy: SE mode. On the external surface of the colony, the sample appears like a pile of sclerites (scale bar 50 µm). **(C–E)** Scanning electron microscopy: BSE mode on polished samples. **(C)** Longitudinal section of a colony. It is possible to observe the emerging axial skeleton (Sk) and, around it, sclerites (white arrows) enclosed in the living tissues (scale bar 200 µm). **(D)** Enlargement of C displaying sclerites within the rising skeleton and free sclerites (white arrows) (scale bar 80 µm). **(E)** Transversal section showing geometrically complex layering (white line) and sclerites embedded in the axial skeleton (white arrows) (scale bar 60 µm). **(F, G)** Micro-X-ray tomography of a 2-year-old settler. The different images represent two sections of the same sample obtained by processing the 3D images acquired with the tomography. **(F)** The voids represent the cavities previously occupied by the polyps (indicated by asterisks) and their organic tissues (Ot: Organic tissue). **(G)** It is possible to observe the axial skeleton (the homogenous white structure, Sk) and the sclerites (the white spots indicated by a dotted circle, Sc) distributed around it. M, mouth; Or, oral; Ab, aboral (scale bar: 1 mm).

10.3389/fmars.2023.1052854

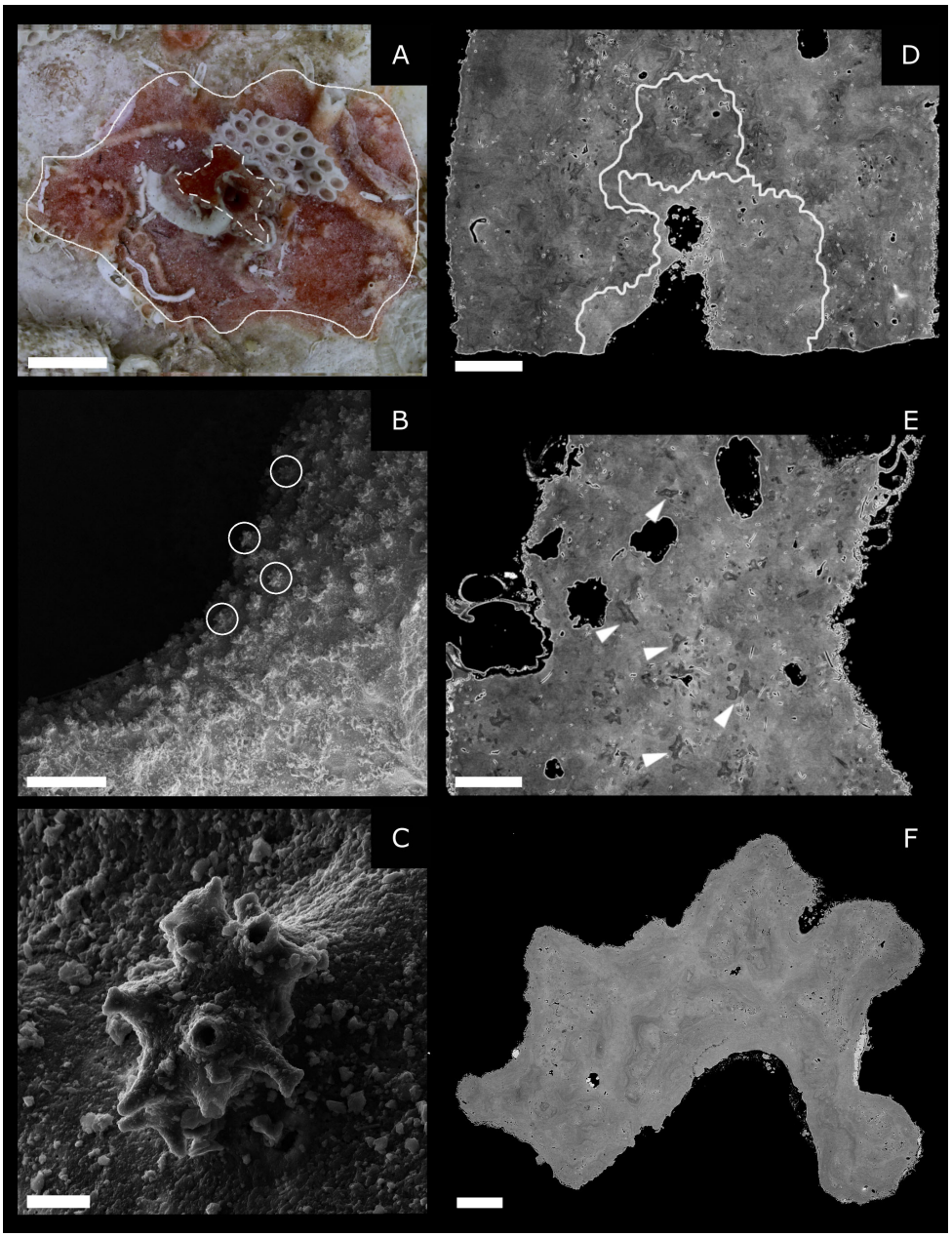

FIGURE 5
3- to 4-year-old samples. **(A)** Stereomicroscope top-down view showing the axial skeleton of the colony (dashed white lines) and the area constituted by diffused sclerites around it (continuous white line) (scale bar 2 mm). **(B, C)** Scanning electron microscopy: SE mode. **(B)** The colony's surface with external micro-protuberances (circles) (scale bar 100 µm). **(C)** blow-up on a single damaged but still recognizable micro-protuberance (scale bar 5 µm). **(D, E)** Longitudinal sections of the axial skeleton of 3- to 4-year-old samples observed by SEM in BE mode (polished sample). The white line indicates the calcitic layers forming the skeleton. White arrows indicate sclerites embedded in the cement (scale bar 200 µm). **(F)** Transversal section of the axial skeleton of a 3- to 4-year-old sample observed by SEM in BE mode (polished sample). No visible annular rings is observed (scale bar 200 µm).

skeletons that we analyzed do not correspond to compositions characteristic of the annular zone (see Supplementary Material 1).

4 Discussion

Our results add to a body of research on octocorals in general (Dunkelberger and Watabe, 1974; Kingsley, 1984; Goldberg and Benayahu, 1987; Kingsley et al., 1987; Jeng et al., 2011), and *C. rubrum* in particular (Grillo et al., 1993; Debreuil et al., 2012; Perrin et al., 2015), shedding light on 1) the role of sclerites during the early stages of life 2) the timing of skeleton formation during the first four years of *C. rubrum* life (Figure 6).

4.1 Role of sclerites during the early stage of life

C. rubrum is an internal brooder that releases larvae that, after the settlement and metamorphosis process, start an extensive tissue

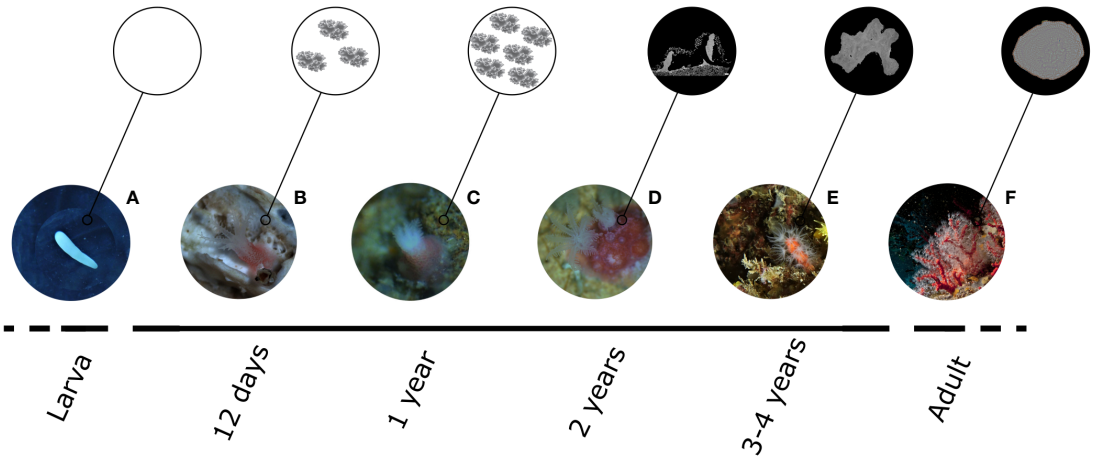

FIGURE 6
Summary of results describing the biomineralization process in *C. rubrum*, from larval to adult stage. **(A)** During the pelagic larval phase, no biomineral structures are present, and larvae are mainly composed of lipids. **(B)** Sclerites start to be produced during the first days after settlement and are detectable in 12-day-old recruits for the first time. **(C)** During the first year of life the only biomineral structure of the recruits is represented by sclerite which number and density increase all along the first year after settlement. At this stage, no cemented skeleton is detectable. **(D)** The presence of an axial skeleton is observed for the first time in 2-year-old recruits. **(E)** 3-4-year-old colonies do not show the presence of growth rings in the skeleton, meaning that the annular growth still does not occur. **(F)** The internal structure of the axial skeleton in adult clonies is organized in two distinct areas: a central medullar zone and a surrounding annular zone constituted by several concentric calcitic layers.

remodeling together with the beginning of calcification through the production of sclerites (Lacaze-Duthiers, 1864). Our results show that sclerites are produced by the primary polyp as soon as 12 days after settlement. For this reason, we hypothesize that the work of mineralization begins earlier than that, probably during the very first days after the settlement, since small forming sclerites may not be optically detectable in younger settlers. Previous research on *C. rubrum* showed that sclerites are made of a dominant inorganic fraction of Mg-calcite associated with a small organic fraction composed of macromolecules (mainly proteins, polysaccharides, and glycoproteins) (Debreuil et al., 2012). Sclerite growth occurs within scleroblasts cells through the secretion of $CaCO_3$ layers (Grillo et al., 1993; Le Goff et al., 2017). Growth rings in sclerites, associated with variations in chemical compositions and concentrations of organic matter, have already been observed in the Mediterranean red coral (Grillo et al., 1993; Floquet and Vielzeuf, 2011; Perrin et al., 2015). Because fully matured sclerites form rapidly (faster than 12 days), the most probable temporal cycle driving the formation of sclerite growth rings is the solar day (and necessarily not the lunar month or annual cycle). Thus, the three to four prominent growth marks observed in sclerites suggest that fully matured sclerites grow in 3 to 4 days. On the other hand, the fainter marks between the main growth rings may indicate the presence of different cycles, possibly linked to the internal dynamics of biomineral growth (e.g., competition between mineral growth and diffusion of the elements in the solution, see Vielzeuf et al., 2018 for a discussion). These results are consistent with previous observations on the high turnover rate of sclerites, which are produced three times faster than the axial skeleton of adult colonies (Allemand and Grillo, 1992).

We showed that sclerites are the only biomineral structure produced by polyps during the first years of life. Until two years, the only biomineral change that occurs is the increase in the number and density of the sclerites. In addition, we observed that the structure formed by sclerites in the young (<2 years) primary polyps did not collapse when the samples dried and that it preserved the shape of the cavity occupied by the polyp. This observation suggests that when the living primary polyp retracts, sclerites form a self-supportive, nearly continuous though deformable protective biomineral armor. Thus, the principal function of sclerites in young *C. rubrum* individuals (<2 years) would be to accompany and protect the fast growth of the young colonies from threats such as abrasion and predation. Furthermore, we showed that in one-year-old recruits, sclerites are not present between the base of the polyp and the substrate, meaning that, before the age of two years, the attachment to the substrate depends exclusively on organic tissues.

On the contrary, in two-year-old corals, a thin calcitic layer -connected to the emerging consolidated skeleton- can be observed at the colony's base in contact with the substrate allowing a firm -and inorganic- anchoring. Furthermore, a stronger attachment to the substrate, which might enhance corals' survival, seems to be provided by sclerites' radial diffusion around the bases of the colonies, according to age. We showed how sclerites are closely distributed around the primary polyp in 1-year-old individuals. Conversely, in older corals (2- and 3-4-year-old), sclerites occupy a progressively wider area around polyps.

4.2 Timing of *C. rubrum* growth

Several studies have focused on the biomineralization processes in adult colonies (e.g., Allemand and Grillo, 1992; Grillo et al., 1993; Vielzeuf et al., 2008; Vielzeuf et al., 2010; Le Goff et al., 2017), but only Lacaze-Duthiers (1864) tried to investigate the skeleton formation of juveniles (Vielzeuf et al., 2022). As seen earlier, after developing a flexible non-consolidated proto-skeleton only formed by sclerites, the first evidence of a consolidated axial skeleton is recorded in 2-year-old colonies. Lacaze-Duthiers (1864), (Figure 111 in pl XIX) described the emerging skeleton as 'horseshoe-shaped", usually higher towards the middle. Interestingly, the same author raised the question of how an

almost circular blade around a polyp can become the medullary zone in the center of the skeleton. According to his interpretation, a clone of the primary polyp appears rapidly and becomes quickly as large as the first one. The second polyp opposes the convexity of its skeleton to that of the first, from which emerges a centered skeleton (X-shaped) in which other clones can lodge. An annular zone will eventually surround this medullary zone. In agreement with Lacaze-Duthiers, and based on our observations, we consider that the beginning of sclerites cementation and the change of shape of the proto-skeleton is triggered by the addition of new polyps, which triplicate in 1 year, passing from 2 ± 1 to 6 ± 1 polyps in 1-year- and 2-year-old individuals, respectively (Kahramanoğulları et al., 2022). It is worth noticing that the skeleton of 2- to 4-year-old individuals presents the same organization as the medullary zone of adult colonies: sclerites embedded within a large proportion of thin layers of calcitic cement. Thus, a similar process of skeleton formation between young colonies and adults' apexes can be expected. Observations on 3-4-year-old corals showed that as a colony grows, the deposited layers become less chaotic, more continuous, and involve fewer and fewer sclerites. At the same time, regularly spaced micro protuberances, appear at the surface of the layers. Perrin et al. (2015) and Vielzeuf et al. (2018) proposed that the micro-protuberances at the skeleton's surface are the calcifying epithelium's footprint. Consequently, a continuous epithelium at the skeleton's surface would appear 3 to 4 years after settlement.

The present study does not allow dating the formation of an annular zone around the skeleton (or medullary zone), nor by SEM observations or LA-ICPMS analysis. Vielzeuf et al. (2018) compared the chemical compositions of the medullary and annular zones by LA-ICPMS, and demonstrated that the concentrations of Li, Na, Mg, Sr, U, were higher in the MZ (slow growth rate) than in the AZ (fast growth rate). These authors attributed the differences in composition to kinetic effects on the incorporation of elements in calcite and noted that the two most discriminating elements are Li and U (see Vielzeuf et al., 2018 their Figure 7D). According to this study, MZ would be characterized by Li and U contents greater than 3 and 0.08 µg/g, respectively. In the present work, LA-ICPMS analyses show that the chemical composition of 3-4-year-old colonies matches those of the medullary zones (not the annular zones), being Li and U higher than the critical values discussed above. Perrin et al. (2015) linked the formation of an annular zone to the presence of a network of deep gastrodermal canals, themselves associated with the presence of regular crenulations at the surface of the skeleton. Crenulations were not observed at the surface of the skeletons that we studied, which corroborates the conclusion that no annular zone formed before 3 to 4 years of age. This result is also consistent with the conclusion of Marschal et al. (2004), who proposed, based on field observations, that *C. rubrum* does not produce growth rings until 3-4 years of age.

4.3 Implications on *C. rubrum* conservation and restoration

Corals, like most benthic marine organisms, suffer high mortality rates during and soon after settlement (Ritson-Williams et al., 2009), which can strongly affect their demography (Santangelo et al., 2007; Bramanti et al., 2009). Coral recruits can die from a myriad of causes, including chronic disturbances such as competition and predation (Mumby, 2006; Smith et al., 2006; Adjeroud et al., 2007) and punctual disturbances such as physical perturbations or diseases (Rylaarsdam, 1983; Connell et al., 1997; Bramanti et al., 2005; Gleason and Hofmann, 2011). In *C. rubrum*, the absence of a hard skeleton, and the lack of a firm attachment to the substratum in early stages, suggest a high vulnerability of these individuals (< two-year-old), making the early life stages dramatically exposed to competition and predation or physical disturbances. From a conservation and restoration point of view, understanding the causes of vulnerability is critical for developing successful restoration plans. As red coral represents an economically valuable resource, the possibility of active restoration should be considered. For species characterized by long life cycles (> 100 years), such as *C. rubrum*, transplantation techniques, widely applied for tropical corals, might not be the most efficient solution. In these cases, nature-based solutions should represent a more efficient alternative as they are based on a life trait of the species (i.e., the production of a high number of larvae) and focused on boosting a natural process (i.e. the post-settlement survival). These techniques should be grounded on understanding the causes of high early mortality, which is considered a major demographic bottleneck. We found a temporal window of vulnerability (0-2 years), during which *C. rubrum's* recruits are small, lack a rigid axial skeleton and are not firmly attached to the substrate. This insight will be pivotal in developing active restoration plans based on sexual reproduction.

Data availability statement

The original contributions presented in the study are included in the article/Supplementary Material. Further inquiries can be directed to the corresponding author.

Author contributions

LB, DV, and BG conceived and designed the study. Material preparation, data collection and analysis were performed by BG, LB, JP, and DV. BG wrote the first draft of the manuscript, and all authors commented on the following versions. All authors contributed to the article and approved the submitted version.

Funding

BG was financially supported by University "La Sapienza" and the ERASMUS+ program. This work benefits from the support of Prince Albert II of Monaco Foundation, and was further supported by the Centre National de la Recherche Scientifique (CNRS), the Institut National des Sciences de l'Univers (INSU) and the Agence Nationale pour la Recherche (ANR) through ANR MOBi 2018-2022. This is contribution ANR MOBi no. 9.

Acknowledgments

The authors gratefully acknowledge F. Bedu and J.L. Devidal for their help with SEM and LA-ICP-MS analyses, respectively; E. Peru

for the technical support and the aquarium system set up, B. Hesse, JC Roca, and the boat crew for the support during SCUBA diving operations. A special thanks to Prof G. Ardizzone for his support during the whole master thesis project. We acknowledge SOLEIL synchrotron for financial support concerning inhouse beamtime. ANATOMIX is an Equipment of Excellence (EQUIPEX) funded by the Investments for the Future program of the French National Research Agency (ANR), project NanoimagesX, grant no. ANR-11-EQPX-0031.

Conflict of interest

The authors declare that the research was conducted in the absence of any commercial or financial relationships that could be construed as a potential conflict of interest.

Publisher's note

Supplementary material

The Supplementary Material for this article can be found online at: https://www.frontiersin.org/articles/10.3389/fmars.2023.1052854/full#supplementary-material

SUPPLEMENTARY MATERIAL 1
Table of the LA-ICPMS analysis of *C. rubrum* 3-4-years-old and adult colonies (AZ and MZ; from Vielzeuf et al., 2018), the statistical methods used to investigate this dataset, and PCA results.

References

Abbiati, M., Buffoni, G., Caforio, G., Di Cola, G., and Santangelo, G. (1992). Harvesting, predation and competition effects on a red coral population. *Neth. J. Sea Res.* 30, 219–228. doi: 10.1016/0077-7579(92)90060-R

Adjeroud, M., Penin, L., and Carroll, A. (2007). Spatio-temporal heterogeneity in coral recruitment around moorea, French Polynesia: Implications for population maintenance. *J. Exp. Mar. Biol. Ecol.* 341, 204–218. doi: 10.1016/j.jembe.2006.10.048

Allemand, D., and Bénazet-Tambutté, S. (1996). Dynamics of calcification in the mediterranean red coral,*Corallium rubrum* (Linnaeus) (Cnidaria, octocorallia). *J. Exp. Zool.* 276, 270–278. doi: 10.1002/(SICI)1097-010X(19961101)276:4<270::AID-JEZ4>3.0.CO;2-L

Allemand, D., Cuif, J. P., Watabe, N., Oishi, M., and Kawaguchi, T. (1994). *The organic matrix of skeletal structures of the Mediterranean red coral, Corallium rubrum*. (Monaco: Bulletin de l'Institut océanographique), 129–139.

Allemand, D., and Grillo, M.-C. (1992). Biocalcification mechanism in gorgonians:45Ca uptake and deposition by the Mediterranean red coral *Corallium rubrum*. *J. Exp. Zool.* 262, 237–246. doi: 10.1002/jez.1402620302

Bayer, F. M. (1955). Contributions to the nomenclature, systematics, and morphology of the octocorallia. *Proc. U. S. Natl. Mus.* 105, 207–220. doi: 10.5479/si.00963801.105-3357.207

Bayer, F. M. (1957). Recent octocorals, in: Geological society of America memoirs. *Geol. Soc. Am.* 67V1, 1105–1108. doi: 10.1130/MEM67V1-p1105

Bramanti, L., Iannelli, M., and Santangelo, G. (2009). Mathematical modelling for conservation and management of gorgonians corals: Youngs and olds, could they coexist? *Ecol. Modell.* 220, 2851–2856. doi: 10.1016/j.ecolmodel.2009.01.031

Bramanti, L., Magagnini, G., De Maio, L., and Santangelo, G. (2005). Recruitment, early survival and growth of the Mediterranean red coral *Corallium rubrum* (L 1758), a 4-year study. *J. Exp. Mar. Biol. Ecol.* 314, 69–78. doi: 10.1016/j.jembe.2004.08.029

Bramanti, L., Vielmini, I., Rossi, S., Tsounis, G., Iannelli, M., Cattaneo-Vietti, R., et al. (2014). Demographic parameters of two populations of red coral (*Corallium rubrum* l. 1758) in the north Western Mediterranean. *Mar. Biol.* 161, 1015–1026. doi: 10.1007/s00227-013-2383-5

Conci, N., Vargas, S., and Wörheide, G. (2021). The biology and evolution of calcite and aragonite mineralization in octocorallia. *Front. Ecol. Evol.* 9. doi: 10.3389/fevo.2021.623774

Connell, J. H., Hughes, T. P., and Wallace, C. C. (1997). A 30-year study of coral abundance, recruitment, and disturbance at several scales in space and time. *Ecol. Monogr.* 67, 461–488. doi: 10.1890/0012-9615(1997)067[0461:AYSOCA]2.0.CO;2

Costantini, F., Taviani, M., Remia, A., Pintus, E., Schembri, P. J., and Abbiati, M. (2010). Deep-water corallium rubrum (L. 1758) from the Mediterranean Sea: preliminary genetic characterisation. *Mar. Ecol.* 31, 261–269. doi: 10.1111/j.1439-0485.2009.00333.x

Debreuil, J., Tambutté, É., Zoccola, D., Deleury, E., Guigonis, J.-M., Samson, M., et al. (2012). Molecular cloning and characterization of first organic matrix protein from sclerites of red coral, *Corallium rubrum*. *J. Biol. Chem.* 287, 19367–19376. doi: 10.1074/jbc.M112.352005

Debreuil, J., Tambutté, S., Zoccola, D., Segonds, N., Techer, N., Marschal, C., et al. (2011). Specific organic matrix characteristics in skeletons of corallium species. *Mar. Biol.* 158, 2765–2774. doi: 10.1007/s00227-011-1775-7

Dunkelberger, D. G., and Watabe, N. (1974). An ultrastructural study on spicule formation in the pennatulid colony renilla reniformis. *Tissue Cell* 6, 573–586. doi: 10.1016/0040-8166(74)90001-9

Floquet, N., and Vielzeuf, D. (2011). Mesoscale twinning and crystallographic registers in biominerals. *Am. Mineral* 96, 1228–1237. doi: 10.2138/am.2011.3805

Gallmetzer, I., Haselmair, A., and Velimirov, B. (2010). Slow growth and early sexual maturity: Bane and boon for the red coral *Corallium rubrum*. estuar. *Coast. Shelf Sci.* 90, 1–10. doi: 10.1016/j.ecss.2010.04.018

Gao, S., Liu, X., Yuan, H., Hattendorf, B., Günther, D., Chen, L., et al. (2002). Determination of forty two major and trace elements in USGS and NIST SRM glasses by laser ablation-inductively coupled plasma-mass spectrometry. *Geostand. Newsl.* 26, 181–196. doi: 10.1111/j.1751-908X.2002.tb00886.x

Garrabou, J., and Harmelin, J. G. (2002). A 20-year study on life-history traits of a harvested long-lived temperate coral in the NW Mediterranean: insights into conservation and management needs. *J. Anim. Ecol.* 71, 966–978. doi: 10.1046/j.1365-2656.2002.00661.x

Gleason, D. F., and Hofmann, D. K. (2011). Coral larvae: From gametes to recruits. *J. Exp. Mar. Biol. Ecol.* 408, 42–57. doi: 10.1016/j.jembe.2011.07.025

Goldberg, W. M., and Benayahu, Y. (1987). Spicule formation in the gorgonian coral pseudoplexaura flagellosa. 1: Demonstration of intracellular and extracellular growth and the effect of ruthenium red during decalcification. *Bull. Mar. Sci.* 40, 17.

Grillo, M.-C., Goldberg, W. M., and Allemand, D. (1993). Skeleton and sclerite formation in the precious red coral *Corallium rubrum*. *Mar. Biol.* 117, 119–128. doi: 10.1007/BF00346433

Jeng, M.-S., Huang, H.-D., Dai, C.-F., Hsiao, Y.-C., and Benayahu, Y. (2011). Sclerite calcification and reef-building in the fleshy octocoral genus sinularia (Octocorallia: Alcyonacea). *Coral Reefs* 30, 925–933. doi: 10.1007/s00338-011-0765-z

Kahramanoğulları, O., Giordano, B., Perrin, J., Vielzeuf, D., and Bramanti, L. (2022). Stochastic diffusion characterises early colony formation in Mediterranean coral *Corallium rubrum*. *J. Theor. Biol.* 553, 111247. doi: 10.1016/j.jtbi.2022.111247

Kingsley, R. J. (1984). Spicule formation in the invertebrates with special reference to the gorgonian leptogorgia virgulata. *Am. Zool.* 24, 883–891. doi: 10.1093/icb/24.4.883

Kingsley, R. J., Bernhardt, A. M., Wilbur, K. M., and Watabe, N. (1987). Scleroblast cultures from the gorgonianLeptogorgia virgulata (Lamarck) (Coelenterata: Gorgonacea). *In Vitro Cell. Dev. Biol.* 23, 297–302. doi: 10.1007/BF02623713

Lacaze-Duthiers, H. (1864). Histoire naturelle du corail: Organisation - reproduction - pêche en Algérie - industrie et commerce. *J. B. Baillière.*

Le Goff, C., Tambutté, E., Venn, A. A., Techer, N., Allemand, D., and Tambutté, S. (2017). *In vivo* pH measurement at the site of calcification in an octocoral. *Sci. Rep.* 7, 11210. doi: 10.1038/s41598-017-10348-4

Lewis, J. C., and Wallis, E. V. (1991). The function of surface sclerites in gorgonians (Coelenterata, octocorallia). *Biol. Bull.* 181, 275–288. doi: 10.2307/1542099

Lowenstam, H. A., and Weiner, S. (1989). *On biomineralization* (Oxford University Press).

Marschal, C., Garrabou, J., Harmelin, J. G., and Pichon, M. (2004). A new method for measuring growth and age in the precious red coral *Corallium rubrum* (L.). *Coral Reefs* 23, 423–432. doi: 10.1007/s00338-004-0398-6

Mumby, P. J. (2006). The impact of exploiting grazers (Scaridae) on the dynamics of Caribbean coral reefs. *Ecol. Appl.* 16, 747–769. doi: 10.1890/1051-0761(2006)016[0747:TIOEGS]2.0.CO;2

Perrin, J., Vielzeuf, D., Ricolleau, A., Dallaporta, H., Valton, S., and Floquet, N. (2015). Block-by-block and layer-by-layer growth modes in coral skeletons. *Am. Mineral* 100, 681–695. doi: 10.2138/am-2015-4990

Priori, C., Mastascusa, V., Erra, F., Angiolillo, M., Canese, S., and Santangelo, G. (2013). Demography of deep-dwelling red coral populations: Age and reproductive structure of a highly valued marine species. *Estuar. Coast. Shelf Sci.* 118, 43–49. doi: 10.1016/j.ecss.2012.12.011

Ritson-Williams, R., Arnold, S., Fogarty, N., Steneck, R. S., Vermeij, M., and Paul, V. J. (2009). New perspectives on ecological mechanisms affecting coral recruitment on reefs. *Smithson Contrib. Mar. Sci.* 38, 437–457. doi: 10.5479/si.01960768.38.437

Rossi, S., Bramanti, L., Gori, A., and Orejas, C. (2017). "An overview of the animal forests of the world," in *Marine animal forests*. Eds. S. Rossi, L. Bramanti, A. Gori and C. Orejas (Cham: Springer International Publishing), 1–26. doi: 10.1007/978-3-319-17001-5_1-1

Rylaarsdam, K. (1983). Life histories and abundance patterns of colonial corals on Jamaican reefs. *Mar. Ecol. Prog. Ser.* 13, 249–260. doi: 10.3354/meps013249

Santangelo, G., Bramanti, L., and Iannelli, M. (2007). Population dynamics and conservation biology of the over-exploited Mediterranean red coral. *J. Theor. Biol.* 244, 416–423. doi: 10.1016/j.jtbi.2006.08.027

Santangelo, G., Carletti, E., Maggi, E., and Bramanti, L. (2003). Reproduction and population sexual structure of the overexploited Mediterranean red coral *Corallium rubrum*. *Mar. Ecol. Prog. Ser.* 248, 99–108. doi: 10.3354/meps248099

Shaheen, M., Gagnon, J. E., Yang, Z., and Fryer, B. J. (2008). Evaluation of the analytical performance of femtosecond laser ablation inductively coupled plasma mass spectrometry at 785 nm with glass reference materials. *J. Anal. At. Spectrom.* 23, 1610–1621. doi: 10.1039/B809880H

Smith, J. E., Shaw, M., Edwards, R. A., Obura, D., Pantos, O., Sala, E., et al. (2006). Indirect effects of algae on coral: algae-mediated, microbe-induced coral mortality. *Ecol. Lett.* 9, 835–845. doi: 10.1111/j.1461-0248.2006.00937.x

van Achterbergh, E., Griffin, W. L., and Stiefenhofer, J. (2001). Metasomatism in mantle xenoliths from the letlhakane kimberlites: estimation of element fluxes. *Contrib. Mineral Petrol.* 141, 397–414. doi: 10.1007/s004100000236

Vielzeuf, D., Allemand, D., Shick, M., Arnaud, V., Bodin, S., and Bramanti, L. (2022). The biology and biomineralogy of the red coral: The Lacaze-Duthiers legacy. *Vie et Milieu / Life & Environment*. 72 (3)

Vielzeuf, D., Floquet, N., Chatain, D., Bonnete, F., Ferry, D., Garrabou, J., et al. (2010). Multilevel modular mesocrystalline organization in red coral. *Am. Mineral* 95, 242–248. doi: 10.2138/am.2010.3268

Vielzeuf, D., Gagnon, A. C., Ricolleau, A., Devidal, J.-L., Balme-Heuze, C., Yahiaoui, N., et al. (2018). Growth kinetics and distribution of trace elements in precious corals. *Front. Earth Sci.* 6. doi: 10.3389/feart.2018.00167

Vielzeuf, D., Garrabou, J., Baronnet, A., Grauby, O., and Marschal, C. (2008). Nano to macroscale biomineral architecture of red coral (*Corallium rubrum*). *Am. Mineral* 93, 1799–1815. doi: 10.2138/am.2008.2923

Vielzeuf, D., Garrabou, J., Gagnon, A., Ricolleau, A., Adkins, J., Günther, D., et al. (2013). Distribution of sulphur and magnesium in the red coral. *Chem. Geol.* 355, 13–27. doi: 10.1016/j.chemgeo.2013.07.008

Weitkamp, T., Scheel, M., Giorgetta, J. L., Joyet, V., Roux, V. L., Cauchon, G., et al. (2017). "The tomography beamlineANATOMIXat synchrotron SOLEIL," in *J. Phys. Conf. Ser*, Vol. 849. 012037. doi: 10.1088/1742-6596/849/1/012037

Weitkamp, T., Scheel, M., Perrin, J., Roux, V. L., Joyet, V., Chaouchi, S., et al. (2018). Progress in microtomography at the ANATOMIX beamline of synchrotron soleil. *Microsc. Microanal.* 24, 244–245. doi: 10.1017/S1431927618013570

Zelli, E., Quéré, G., Lago, N., Di Franco, G., Costantini, F., Rossi, S., et al. (2020). Settlement dynamics and recruitment responses of Mediterranean gorgonians larvae to different crustose coralline algae species. *J. Exp. Mar. Biol. Ecol.* 530–531, 151427. doi: 10.1016/j.jembe.2020.151427